ASCE

Morphological, Thermal, and Mechanical Properties of Asphalt Binders Modified by Graphene and Carbon Nanotube

Xiaokong Yu[1]; Mehdi Zadshir, S.M.ASCE[2]; Jessie Ruixuan Yan[3]; and Huiming Yin[4]

Abstract: The mechanical behavior of asphalt concrete varies with temperature; therefore, researchers have been developing technologies to reduce temperature fluctuations in pavement overlays. Increasing the thermal conductivity of asphalt concrete is a key component in the realization of these technologies. Previous studies have introduced, among other additives, carbon nanotubes (CNTs), graphite, graphene nanoplatelets (GNPs), and copper slag to asphalt binders/concrete to enhance their thermal-physical properties. However, it has been challenging to assess the distribution of these additives in asphalt materials. In this paper, binary (i.e., binder/CNT and binder/GNP) and ternary (i.e., binder/CNT/GNP) composites were prepared by pretreating the additives with a surfactant and through sonication, before they were mixed into the hot binder using a mechanical shear mixer. Morphology and dispersion uniformity of CNTs and GNPs in the binders were evaluated using a digital microscope and scanning electron microscopy (SEM). The thermal conductivity of these samples was measured using Nanoflash combined with differential scanning calorimetry. The rheological properties were tested using rheometry. Results showed that our sample preparation method was able to uniformly disperse the CNTs and GNPs in the binder, as seen in the digital microscope images that offered more representative morphologies of asphalt binders than SEM. The addition of CNTs (0%–2% by weight) and/or GNPs (0%–15% by weight) improved the binder's thermal conductivity at a limited degree, whereas the rheological properties of the CNT/GNP-modified binders remained very close to those of the control sample. Findings from this work may provide some insights into the development of new asphalt materials as well as other CNT/GNP-based composites. **DOI: 10.1061/(ASCE)MT.1943-5533.0004183.**

Author keywords: Asphalt binder; Thermal conductivity; Carbon nanotubes (CNTs); Graphene nanoplatelets (GNPs); Morphology; Rheology; Digital microscope.

Introduction

Asphalt binders (also called bitumens) are widely used in pavement construction, and they act as the glue holding all the aggregates together. Over 94% of the 4.2 million km (2.6 million mi) of paved roads in the US are paved with asphalt concrete (Chen and Yin 2016). However, the strength of asphalt concrete varies with temperature, and the strength decreases beyond its designed working temperature range (Ahmad and Khawaja 2018). In cold climate regions, thermal stresses in asphalt concrete increase exponentially with the loss of ductility when the temperature is low, and thermal contraction becomes significant, leading to thermal cracks in pavements (Dave et al. 2011). In contrast, the asphalt pavements' surface temperature can reach 70°C or higher in the summer in warm or hot climate regions due to the high absorption coefficient of asphalt materials to solar radiation, resulting in thermal oxidation of the material and rutting in pavement overlays (Khan et al. 2019; Pan et al. 2014; Van Bijsterveld et al. 2001).

Therefore, researchers are developing different technologies to reduce temperature fluctuations in asphalt pavements (Athukorallage et al. 2018; Chen et al. 2011a, b; Eugster and Schatzmann 2002; Loomans et al. 2003; Mallick et al. 2012; Manning et al. 2015), among which the most promising one is called hydronic asphalt pavement (HAP). The HAP system consists of a series of pipes embedded in the pavements, control and sensing modules, a heat exchanger, and the thermal conductive pavement overlay (Chen et al. 2011a; He et al. 2019; Mallick et al. 2012). HAP heats the pavement surface for deicing in winter by extracting the heat from underground sources such as geothermal energy and cools down the pavement in summer by dissipating the heat back to the underground source (Eugster and Schatzmann 2002; He et al. 2019; Loomans et al. 2003). Other benefits of the multifunctional HAP system include extending the life span of the pavement as well as reducing pavements' long-term maintenance costs.

One of the challenges encountered in developing an efficient HAP system lies in increasing the thermal conductivity of asphalt concrete in order to better facilitate the thermal energy transfer in the asphalt pavement. To improve the thermal conductivity of asphalt materials, previous studies have added carbon nanotubes (CNTs), graphite, graphene nanoplatelets (GNPs), copper slag, and other additives to asphalt binders and/or concrete (Ashish and Singh 2020;

[1]Postdoctoral Research Scientist, Dept. of Civil Engineering and Engineering Mechanics, Columbia Univ., New York, NY 10027. ORCID: https://orcid.org/0000-0002-2165-1481. Email: xiaokongyu@gmail.com

[2]Graduate Research Assistant, Dept. of Civil Engineering and Engineering Mechanics, Columbia Univ., New York, NY 10027. Email: mz2683@columbia.edu

[3]Laboratory Research Assistant, Dept. of Civil Engineering and Engineering Mechanics, Columbia Univ., New York, NY 10027. Email: jry2115@columbia.edu

[4]Associate Professor, Dept. of Civil Engineering and Engineering Mechanics, Columbia Univ., New York, NY 10027 (corresponding author). ORCID: https://orcid.org/0000-0001-6549-9066. Email: hy2251@columbia.edu; yin@civil.columbia.edu

Note. This manuscript was submitted on March 16, 2021; approved on September 10, 2021; published online on February 17, 2022. Discussion period open until July 17, 2022; separate discussions must be submitted for individual papers. This paper is part of the ***Journal of Materials in Civil Engineering***, © ASCE, ISSN 0899-1561.

Bai et al. 2015; Dawson et al. 2012; Latifi and Hayati 2018; Pan et al. 2014; Vo and Park 2017; Wang et al. 2016). These additives all have much higher thermal conductivity than conventional asphalt binders and asphalt concrete, and as a result, it is expected that they can improve the thermal conductivity of modified asphalt materials. For instance, the thermal conductivity of single-walled and multiwalled CNTs can reach 7,000 and 3,000 W/mK (Berber et al. 2000), respectively, whereas the upper limit for the thermal conductivity of the conventional asphalt binders and asphalt concrete is 1–2 W/mK (Pan et al. 2014; Vo and Park 2017).

However, the effectiveness of improving the thermal conductivity of asphalt materials by adding CNTs, GNPs, and other conductive fillers depends on many factors. First, the dispersion uniformity of these additives in the matrix affects the heat transfer in the composites. CNTs and GNPs tend to agglomerate in the matrix due to the strong van der Waals interactions within the nanotubes/particles (Ashish and Singh 2020; Du and Dai Pang 2018; Han and Fina 2011; Kinloch et al. 2018). Studies have revealed a decreasing trend in the thermal conductivity of asphalt concrete when the clustering of additives was present (Vo and Park 2017). To facilitate the dispersion of CNTs in a matrix, techniques such as ultrasonication, surfactant-assisted processing, and functionalization of the CNTs have been used (Du and Dai Pang 2018; Paredes and Burghard 2004).

Second, how these high-aspect-ratio additives (i.e., the mixing methods) and at what dosages are added into asphalt binders significantly affect the additives' distribution in the matrix. For instance, researchers reported that the wet-mixing method (i.e., the additives are first dispersed in a liquid medium and then added to the asphalt binder) offered a better dispersion of CNTs in the binder and thus a higher thermal conductivity of the modified binder compared with the dry-mixing process (i.e., the additives are directly added to the binder) (Bai et al. 2015; Latifi and Hayati 2018). Regarding the optimal concentration of the additives, it was reported that when CNTs or carbon fibers were added at a higher dosage, they tend to bundle together, resulting in a lower thermal conductivity of the composite (Vo and Park 2017).

Third, the formation of an interconnecting network of the conductive fillers in the matrix is desirable for heat transfer in asphalt materials, and therefore more effectively increases the asphalt materials' thermal conductivity. For example, research has demonstrated that the addition of a combination of tubular CNTs/cylindrical carbon fibers and two-dimensional graphite/graphene produced asphalt concrete with thermal conductivity higher than those of specimens modified with any single filler (Bai et al. 2015; Che et al. 2017; Vo and Park 2017). Researchers believed that this was because of the well-developed interconnecting network created by the longitudinal carbon fibers/CNTs and flakelike GNP; however, there was no direct evidence of hybrid CNT/GNP networks.

One can see that the three aforementioned factors are all related to the dispersion and distribution of the additives in asphalt materials; this reveals the importance of discovering the appropriate tools for evaluating the distribution and formation of the interconnecting networks formed by conductive fillers in asphalt materials. Nevertheless, no reliable methods have yet been developed to assess the dispersion and distribution of CNTs, GNPs, or other nanoscale and microscale fillers in asphalt materials, presenting a fundamental challenge to the effective enhancement of asphalt-based materials' thermal conductivity.

Most of the current studies have used a scanning electron microscope (SEM) to study the morphologies of asphalt materials modified with various types of fillers (Ashish and Singh 2020; Bai et al. 2015; Faramarzi et al. 2015; Latifi and Hayati 2018; Vo and Park 2017). However, SEM might not be the ideal tool for such purpose for the following reasons: (1) asphalt materials are not electrically conductive; thus a layer of conductive coating must be applied to the surface of the asphalt sample, which could possibly modify the specimen's original morphology and obscure the nanoscale or microscale fillers from sight (Ashish and Singh 2020); and (2) electron-beam exposure and surface charging may cause the evaporation of volatiles, surface hardening, and certain chemical reactions of the asphalt materials (Lu et al. 2018), therefore artificially creating new surface morphology. Concerned about the limitations of using SEM to evaluate the dispersion of CNTs in asphalt binders, researchers have tried to compare the viscosity of the control binder with CNT-modified ones and used viscosity data as an indirect way of assessing the distribution uniformity of CNTs (Ashish and Singh 2020). Yet the information obtained from such an indirect approach was inadequate because the correlation between the viscosity trend and the distribution of the additives requires further investigation.

This paper aims to provide a more comprehensive evaluation of the effectiveness of adding CNTs and GNPs into asphalt binders for improving binders' thermal conductivity and to explore a heuristic approach of studying the distribution of nanosize and microsized additives in asphalt binders. To achieve these objectives, the authors developed a more sophisticated mixing method and designed an experimental matrix that includes binary (i.e., CNT- or GNP-based binders) and ternary (CNT- and GNP-based binders) composites. The morphologies and the dispersion of additives in the binders were studied using both SEM and a digital microscope. The thermal conductivity of the samples was measured using the flash method combined with differential scanning calorimetry. In addition, the effects of the additives on the binders' rheological properties were evaluated using rheometry. Detailed methods, data analysis, results, and conclusions are given in the subsequent sections.

Materials and Methods

Materials

Neat Binder

The neat binder (PG 64-22) used in this study was provided by Peckham Industries (Bronx, New York). The material has been tested and certified to be in conformance with AASHTO MP 1 (AASHTO 1998) requirements and it is used to pave roads in states including New York, New Jersey, Pennsylvania, and New England according to the DOT specifications (Asphalt Institute 2021). The properties of the neat asphalt binder are given in Table 1.

Multiwalled Carbon Nanotubes

Multiwalled carbon nanotubes (MWCNT) (Stock US4315) were purchased from US Research Nanomaterials (Houston, Texas) and they were manufactured by the chemical vapor deposition method. Table 2 summarizes the relevant properties of the MWCNTs.

Table 1. Specifications of the neat binder

Parameter	Value
Performance grade (PG)	PG64-22
Penetration	65
Elastic recovery	0.00
Mix temperature (maximum/minimum) (°C)	164/157
Compaction temperature (maximum/minimum) (°C)	151/146
Viscosity at 135°C (Pa · s)	493
Viscosity at 165°C (Pa · s)	135
Gravity at 15.6°C	1.043
Gravity at 25°C	1.037

Table 2. Properties of the MWCNTs

Parameter	Properties	Analysis method
Purity	>95% Carbon nanotubes >97% Carbon content	TGA and TEM
Outside diameter	50–80 nm	HRTEM, Raman
Inside diameter	5–15 nm	
Length	10–20 μm	TEM
Specific surface area	>40 m^2/g	
Thermal conductivity	~3,000 W/mK	
Electrical conductivity	>100 s/cm	
Ash	<1.5% by weight	TGA
Tap density	0.18 g/cm^3	
True density	~2.1 g/cm^3	
C	97.37%	EDX spectroscopy
Cl	0.20%	EDX spectroscopy
Fe	0.55%	EDX spectroscopy
Ni	1.86%	EDX spectroscopy
S	0.02%	EDX spectroscopy

Note: EDX = energy-dispersive X-ray; TGA = thermogravimetric analysis; TEM = transmission electron microscope; and HRTEM = high resolution transmission electron microscope.

Graphene Nano Platelets

GNPs were purchased from Cheap Tubes (2019). The GNPs were of Grade 4, with a purity of >99% by weight and a surface area of >700 m^2/g. The thermal conductivity of GNPs is approximately 300 W/mK (Che et al. 2017), and the density is 2.6 g/cm^3.

Dispersant

The dispersant (Stock US4498) was purchased from US Research Nanomaterials (Houston, Texas). According to the information on the vendor's website (US Research Nanomaterials 2021), the dispersant is a nonionic surface active agent, and it contains aromatic groups with a good affinity and the ability to be easily adsorbed on the wall of the carbon nanotubes.

CNT/GNP-Modified Asphalt Binders

Preparation of the CNT/GNP Solutions

When adding CNTs or graphene into a matrix without any treatment, poorly dispersed bundles or agglomerates are often formed in the matrix, which leads to poor interfacial connectivity and severely affected the composite's performance (Kinloch et al. 2018). In this study, CNTs and GNPs were pretreated with the aforementioned mentioned commercial dispersant to overcome their strong van der Waals interaction and then subjected to ultrasonication to achieve a better dispersion in the asphalt binder.

Fig. 1 shows the process of preparing the CNT/GNP solutions. To prepare the CNT solution, 8 g of dispersant was added to 180 g of deionized (DI) water in a glass beaker, and the solution was stirred using a magnetic stirrer for approximately 20 min until the dispersant was completely dissolved. Next, 11 g of CNTs were added to the solution, followed by 30 min of sonication using a Fisher Scientific probe sonicator (model FB505, power output 500 W, and a probe frequency of 20 kHz) with a titanium solid tip of 19.1 mm in diameter. A pulse mode of 70%, with 10 s on and 2 s off was used. During the sonication, the glass beaker was placed in an ice bath to ensure that the temperature of the solution remained below 35°C. The CNT solution prepared this way has a dispersant to CNT ratio of 1:1.375, which is within the recommendation of the manufacturer of the dispersant (Chen et al. 2016).

A similar process was used to prepare the GNP solution. First, 7.2 g of dispersant was added to 300 g of DI water in a glass beaker and stirred until the complete dissolution of the dispersant was reached. Next, 90 g of GNP was added to the solution, followed by 4 h of sonication. Other settings for the sonication process of the GNP solution were the same as those used for the CNT solution. The GNP solution prepared this way has a dispersant to GNP ratio of 1:12.5, which is much lower than the dispersant to CNT ratio in the CNT stock solution to avoid the overuse of dispersant because a higher proportion of GNP than CNT is used.

Preparation of CNT/GNP-Modified Asphalt Binders Using an Oil Bath and Shear Mixer

Previous studies reported that a combination of fillers (e.g., carbon fibers and graphite for asphalt mixture, and expanded graphite and CNT for high-density polyethylene) can form a conductive network and therefore can improve the thermal conductivity and electrical conductivity of the composite more effectively than those with a single type additive (Che et al. 2017; Vo and Park 2017). For this study, we designed our experimental matrix so that we could compare the effects of a single additive (i.e., GNPs or CNTs) with those of a combination of the two additives (i.e., GNPs and CNTs) on asphalt binders' thermal and mechanical properties. We also limited the highest dosages for the GNPs and CNTs to be 15% and 2% by weight, respectively, in accordance with other researchers' practices (Ashish and Singh 2020; Pan et al. 2014; Vo and Park 2017) not only for avoidance of the agglomeration prevalent in higher dosages but also in consideration of the added cost that these additives would require of the asphalt pavement industry. The weight percentages of GNP and CNT with respect to the neat binder were 0%, 10%, and 15%, and 0%, 1%, 1.5%, and 2%, respectively. Fig. 2 shows the samples' notation and their compositions. The highest GNP and CNT dosages were 15% and 2% by weight, translating to 6.44% and 0.98% by volume, respectively.

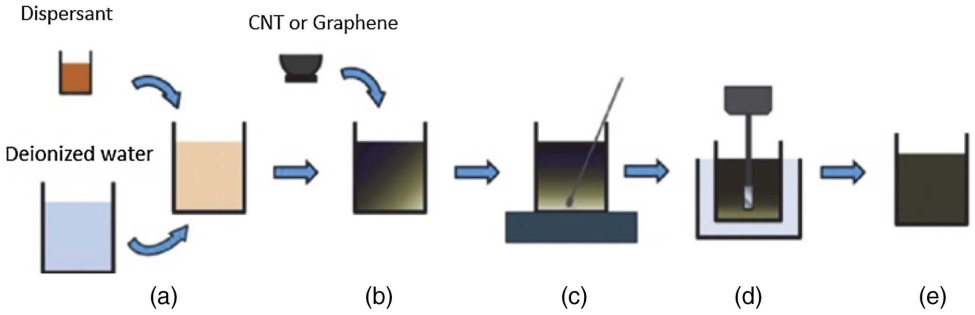

Fig. 1. Preparation process for the CNT and GNP suspensions: (a) preparation of dispersant solvent; (b) addition of CNT or GNP into the solvent; (c) manual stirring the mixture; (d) sonication mixing of the mixture; and (e) uniformly mixed aqueous solution.

J. Mater. Civ. Eng., 2022, 34(5): 04022047

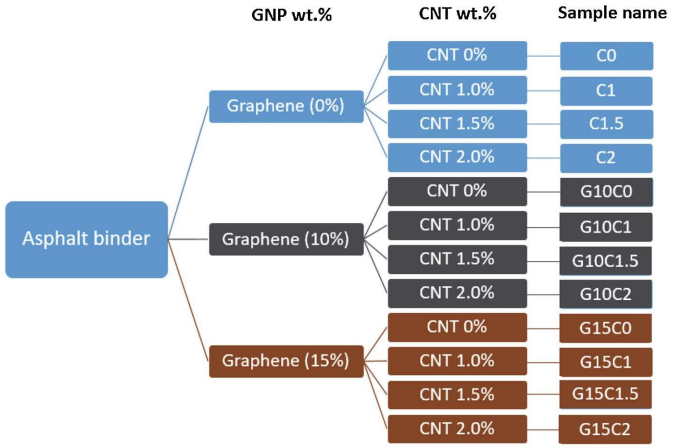

Fig. 2. Sample notation and their compositions.

With the CNT and GNP suspensions prepared, we then used an oil bath and a mechanical shear mixer to achieve a better dispersion and distribution of CNTs/GNPs in the asphalt binder. Fig. 3 shows the mixing setup. The mixing procedure was as follows. An oil bath was heated using a hot plate and maintained at 160°C–180°C (a thermocouple and a thermometer were used to monitor this); Then, 50 g of neat binder, which had been preheated in an oven at 120°C for about an hour, was poured into a stainless-steel beaker and subsequently placed in the oil bath. When the temperature of the binder in the beaker reached ~150°C, the calculated amount of CNT and/or GNP solution was carefully deposited into the asphalt binder using a disposable plastic eyedropper, with the shear mixer rotating at 50 rotation per minute (rpm) (not too fast so as to avoid any splash from the solution being added).

Bubbles were initially generated from the DI water in the CNT/GNP solutions meeting the hot binder and evaporating; they gradually disappeared with continued mixing, and the temperature of the binder decreased to ~105°C due to the heat dissipation caused by the bubbles collapsing. After about 30 min, when there were no longer any significant bubbles visible in the binder and the binder temperature had returned to 140°C–150°C, the speed of the shear mixer was increased to 250 rpm, and mixing continued for 30 min. Once the mixing was completed, the CNT/GNP-modified binders were transferred to aluminum cans and placed in a vacuum oven set at 115°C for about 10 h to remove any remaining water residue. The samples were taken out of the vacuum oven when each sample's weight change before and after putting in the vacuum oven became less than 0.1%.

It should be mentioned that the common practice in the asphalt industry for testing the segregation of a modifier in polymer-modified binders is to perform a separation test known as the cigar tube test. In this test, the aluminum ointment tube is filled with 50 g of modified asphalt binder, and the tubes are sealed and kept in an oven at 163°C for 48 h. Then, the samples are transferred for 4 h. Afterward, the tube is separated into three sections, and the samples at the top and the bottom sections are tested with a dynamic shear rheometer (DSR) for any significant variation in the modulus values. However, in this study, due to the nature of the nanomaterials and their initial dispersion in the surfactant, the separation test was omitted to avoid evaporating the dispersant agent at the extended exposure to high temperature, and instead, the stick test was performed.

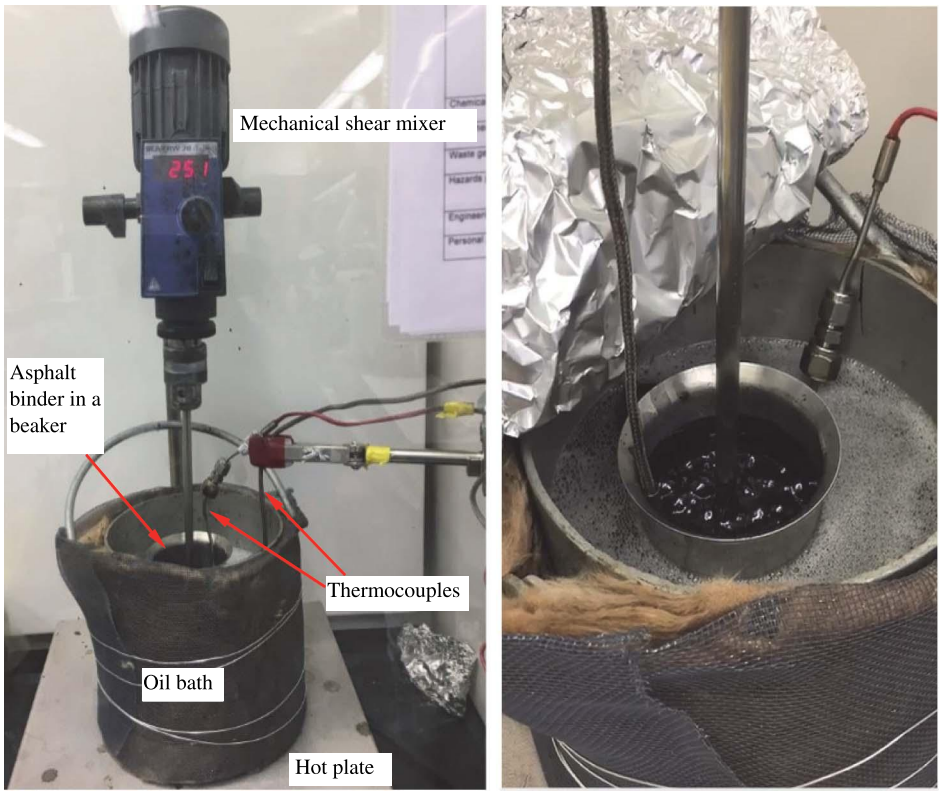

Fig. 3. (a) Setup for mixing the CNT/GNP solutions into the asphalt binder using an oil bath and a mechanical shear mixer; and (b) bubbles generated when the DI water from the CNT/GNP solutions met the hot binder; however, they collapsed and vaporized as the mixing continued.

J. Mater. Civ. Eng., 2022, 34(5): 04022047

To make sure that the nanomodifiers did not settle at the bottom of the beaker afterward, a stick test was used in which a wooden stick was inserted at the bottom of the solution 24 and 48 h after the sonication, and if no residue is observed after the stick is taken out, it was concluded that the solution has been stable and well dispersed.

Characterization

Morphology Using SEM and Digital Microscope

A Zeiss SIGMA VP SEM (Jena, Germany) was used to study the as received GNP powder, CNT, and the binary and ternary asphalt composites. CNTs and GNPs are conductive, and no additional coating is needed when imaged using the SEM. The GNP sample for SEM was prepared by gently pressing a thin layer of GNP powder onto a piece of conductive aluminum tape adhered to an aluminum disk. The CNT sample for SEM was prepared by dropping ~10 μL of CNT solution onto a piece of aluminum plate and then leaving the sample in ambient conditions for at least 24 h in order for the DI water to evaporate. Asphalt samples with CNT/GNP were prepared by butter-spreading a thin layer of hot asphalt onto a piece of silicon wafer. The nonconductive asphalt samples were coated with carbon (a few nanometers in thickness) using a sputter coater to inhibit charging and improve the secondary electron signal in SEM.

A Keyence VHX-5000 (Osaka, Japan) digital microscope, with a VH-Z250T (250× to 2,500×) magnification lens, was also used to study the morphologies of CNT/GNP-modified asphalt binder samples. The VHX has a high depth of field and can create a depth composition image quickly. The high dynamic range (HDR) function allows capturing multiple images by varying the shutter speed to produce a fine detail image.

To obtain repeatable and representative measurements of the morphologies of the binders using the SEM and the digital microscope, two to three specimens were prepared for each type of sample, and at least three images were taken at different locations on the surface of each specimen.

Differential Scanning Calorimetry

A TA Instruments Q250 (New Castle, Delaware) differential scanning calorimeter (DSC) was used to measure the specific heat capacity (C_p), which was used as an input parameter for the Nanoflash for thermal conductivity calculation of the samples. For sample preparation, Tzero hermetic pans and hermetic lids were used to hold ~10 mg of the sample. No further drying process was applied to the samples before sealing the pan. The modulated DSC (MDSC) function was employed because it provides greater sensitivity than regular DSC (Masson et al. 2002; Yu et al. 2019). MDSC heating and cooling curves were obtained with a modulation period of 60 s and an amplitude of ±0.47°C. A nitrogen cooling system was used for cooling, and the nitrogen gas was purged at a rate of 50 mL/min.

All samples were subjected to the following thermal cycles: (1) initial rapid cooling: after being equilibrated at 90°C, the samples were cooled to −80°C at a ramp rate of 10°C/min and then held isothermal for 5 min; (2) first heating from −80°C to 90°C at 4°C/min and then held isothermal for 5 min; (3) first cooling from 90°C to −80°C at 4°C/min and then held isothermal for 5 min; and (4) second heating from −80°C to 90°C at 4°C/min and then held isothermal for 5 min. Specific heat of each sample was determined from the second heating (i.e., Step 4) because this cycle shall give a more stable measurement of the sample's thermal property.

Laser Flash Apparatus

The Nanoflash LFA 447 (Netzsch Instruments, Selb, Germany) was used to measure the thermal diffusivity and thermal conductivity of the asphalt binders according to the flash method and the ASTM E1461-13 (ASTM 2013) standard. The Nanoflash uses a high-performance xenon flash lamp to produce the heat pulse on the rear of the sample. An infrared (IR) detector is placed on top of the sample and collects the heat that is propagated through the sample. A sample holder (Netzsch Instruments) specially designed for liquids with low thermal conductivity was used for our measurements. The sample holder is a set that consists of a round crucible (12.7 mm in diameter) made of 99.9% aluminum, a ring made of stainless steel, and a lid. When assembled, the set gives a spacing of 0.53 mm, and it is recommended to make the sample thickness to be as close to the designed thickness as possible for more accurate measurements. The sample holder is designed for low-thermal-conductivity liquid samples. All samples were tested at 40°C, and 10 to 15 shots were obtained for each sample for statistical analysis at a gain of 5,012 and a medium pulse width.

All analyses were done using the 3-layer heat loss with plus correction model embedded in the Nanoflash analysis software, and fitting to the raw data was limited to the first 5,000 ms. Prior to testing asphalt samples, the instrument was first calibrated by measuring the thermal conductivity of deionized water at 25°C and the results were within 1% deviance from the literature. The thermal conductivity of a specimen can be determined by multiplying the thermal diffusivity by the sample's specific heat and density. The specific heat of the samples was measured using the DSC. Densities of the modified samples were calculated by the mixture rule (assuming no air bubbles within the samples) and the density-mass-volume relationship [i.e., $\rho = m/V = m/\sum(m_i/\rho_i)$].

Dynamic Shear Rheometer

For the rheological properties, a TA Instrument dynamic shear rheometer (DHR-3) was used, and the ASTM D7175-15 (ASTM 2008) standard was applied as a guideline for the preparation of the samples. Oscillation amplitude sweep test and oscillation frequency sweep test were done using the 25-mm-diameter parallel plates with a 1-mm gap. The frequency sweep test was used to obtain the rheological parameters such as G' (elastic or storage modulus), G'' (viscous or loss modulus), G^* (complex modulus), phase angle (δ), and η^* (complex viscosity) of the samples. Test frequencies chosen for each sample were set in the range of 0.1 to 100 rad/s (i.e., 0.0159 to 15.9 Hz) from 28°C to 70°C with a 6°C increment while 1% strain was applied.

Results and Discussion

Morphologies of CNT/GNP-Modified Binders and Dispersion of CNT/GNP in the Binders

Morphologies of CNTs and GNPs Using SEM

SEM morphologies of the CNTs prepared by air-drying the CNT solution and the as-received GNPs are shown in Fig. 4. The CNTs are in wormlike shapes, and their average outer diameter is measured to be 62 ± 9.5 μm, consistent with the values the vendor claimed. There are no obvious CNT agglomerates; therefore, the surfactant combined with sonication worked appropriately to separate the CNTs. The GNPs are two-dimensional flakes that are not perfectly round; the size of the flakes varied but to a small extent, with an average diameter of 2–3 μm.

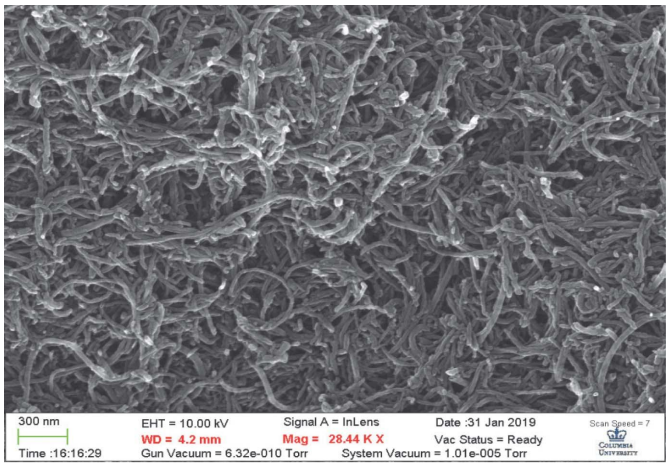

(a)

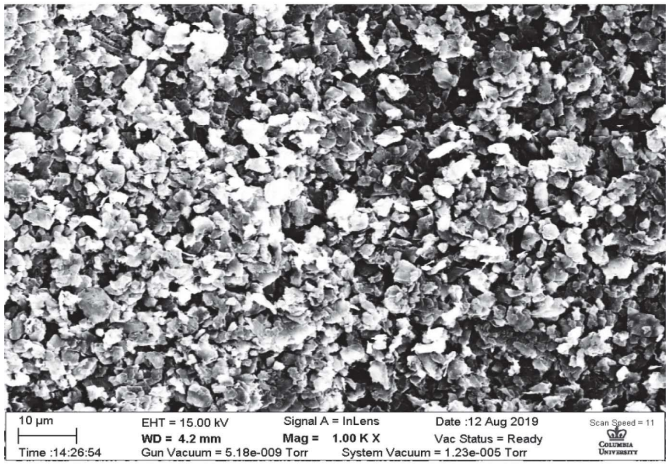

(b)

Fig. 4. SEM images of (a) CNT prepared by air-drying the CNT solution; and (b) as-received GNP.

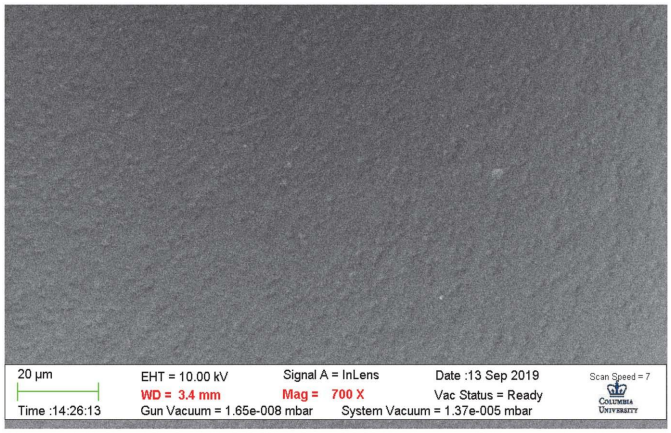

(a)

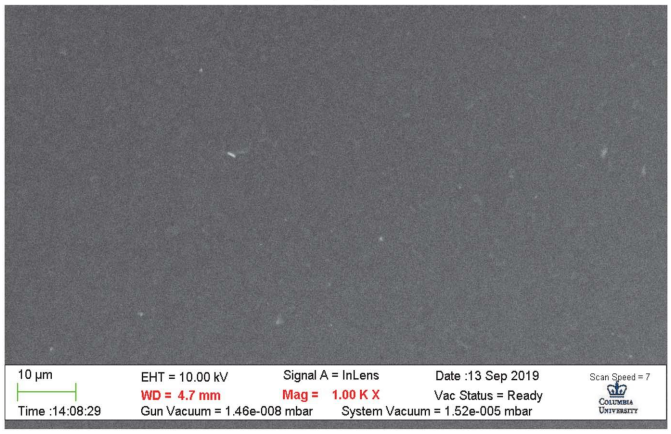

(b)

Fig. 5. SEM images of (a) G10C0; and (b) G15C2.

Is SEM or Digital Microscope More Suitable for Morphological Study of CNT/GNP-Modified Binders?

At first, the authors focused on using SEM to study the morphologies of the CNT/GNP-modified asphalt binders by following what other researchers have done in the past (Ashish and Singh 2020; Bai et al. 2015; Faramarzi et al. 2015; Latifi and Hayati 2018; Vo and Park 2017). However, from analyzing our preliminary results, we learned that it was quite challenging to use SEM to see the CNTs or GNPs in the binary or ternary composites (i.e., binder/CNTs, binder/GNPs, or binder/GNPs/CNTs). Even though we tried to adjust acquisition parameters (e.g., voltage, brightness, contrast, and magnification) to optimize the SEM images, the best images for CNT/GNP-modified samples that we were able to obtain using the SEM are shown in Fig. 5.

As seen in Fig. 5, Sample G10C0 (i.e., 10% by weight GNPs and no CNTs) mainly shows goosebumplike structures of a few micrometers in size, which resemble the pristine GNP flakes [Fig. 4(b)], and this can be further confirmed by the digital microscope images [e.g., Figs. 6(c) and 9]. SEM image of sample G15C2 (i.e., 15% by weight GNP and 2% by weight CNT) is blurry, yet vaguely one can see goosebumplike structures mixed with longitudinallike features that resemble the GNP and CNTs, respectively.

Even though the features in the SEM images in Fig. 5 are visible, they are hard to be quickly identified for someone who does not know this type of samples well. After a long time of trial and error, the authors believed that the SEM is not the appropriate tool to study the morphologies of asphalt materials nor the dispersion uniformity of the CNTs/GNPs in asphalt binders. This is because the conductive coating layer that is required for the SEM sample preparation of nonconductive samples made it very challenging to see the true features on the surfaces of the samples. In other words, the coating could distort the original topographical features on the surfaces of the CNT- and/or GNP-modified asphalt samples.

In order to verify this hypothesis, the authors picked the G15C2 as an example and examined its morphology using both the SEM and digital microscope. SEM Sample G15C2 was coated with the conductive layer, whereas no coating was applied onto the surface of the same sample for the digital microscope because it is not necessary to do so. Fig. 6(a) shows that the surface of the coated G15C2 displayed leathery like patterns with an average lateral size of 10 μm, which is almost 3–5 times the size of the pristine GNP flakes. The zoomed-in image of that exact area [Fig. 6(b)] showed additional colorful particles that are blended in the leather pattern, and these colorful structures are believed to be the CNTs or GNPs. In comparison, surfaces of the G15C2 samples without the conductive coating did not show any leathery or cracklike patterns; instead, the surfaces exhibited colorful diffraction patterns and particlelike features as a result of the light diffraction from the GNP and CNTs that were mixed in the binder [Fig. 6(c)].

The average size of these colorful diffraction patterns was very close to that of the pristine GNP flakes [Fig. 4(b)], and the same patterns were also seen in all other samples modified with GNP and/or CNT. Therefore, the authors concluded that the leatherylike

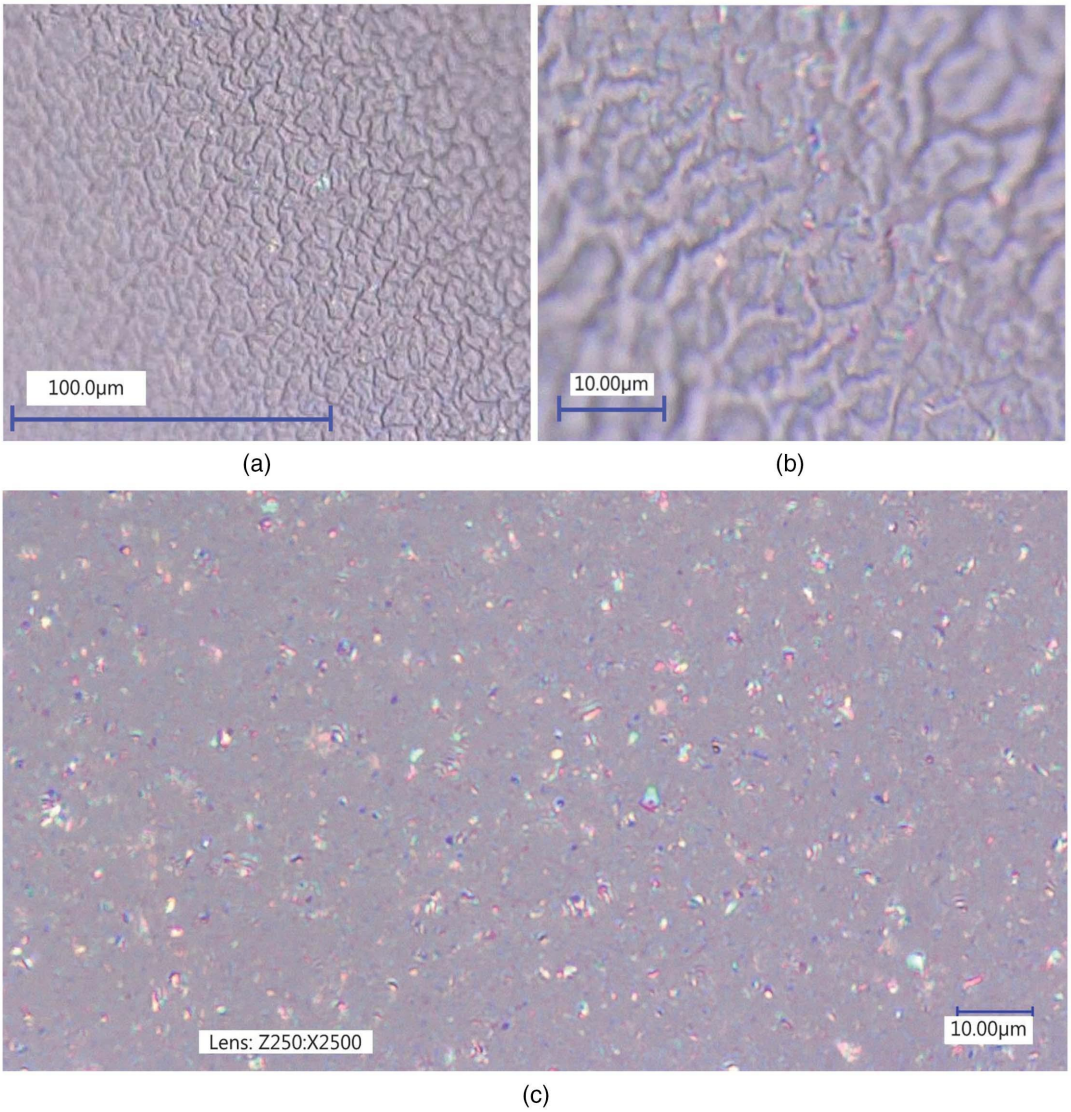

Fig. 6. Digital microscope images of (a) G15C2 with a layer of conductive coating (i.e., the sample prepared for SEM imaging) at a magnification of 500×; (b) the same sample as in plot (a) at a magnification of 2,500×; and (c) G15C2 without any coating at a magnification of 2,500×.

patterns in the coated sample were not the true features on surfaces of GNP/CNT-modified samples; instead, the leathery patterns on surfaces of the coated samples in Figs. 6(a and b) were a result of the conductive carbon coating (a few nanometers thick) filling in some of the topographically lower areas of the GNP/CNT-modified binders and connecting the adjacent GNPs/CNTs. Therefore, from this point forward, we focused on using the digital microscope to characterize the morphologies of all asphalt samples and to evaluate the dispersion uniformity of the GNPs and CNTs in asphalt binders.

Digital Microscope Images of Binders Modified with CNTs Only

The digital microscope has both the conventional image recording function and HDR function. Fig. 7 shows that the HDR mode gives more details of a sample's surface morphology. In this figure, more contrasts can be seen in the HDR image than the one obtained using the regular recording function. Highlighted in the ovals are the CNTs distributed close to the very top of the sample surface and more laterally (i.e., parallel to our view). The dark dots in images of C1, C1.5, and C2 correspond to the areas with a lower height (i.e., sunk into the sample surface) or areas out of the field of depth of the digital microscope.

HDR images of the pure binder (i.e., the control sample, C0) and the CNT-modified binders (i.e., C1, C1.5, and C2) are shown in Fig. 8.

The surface of the control sample, C0, was very smooth and featureless, making it impossible to focus on the surface. To resolve this, the authors used tweezers to poke on the sample's surface, which created the bright dot as highlighted in the rectangle Fig. 8(a). In contrast, surface morphologies of the binder/CNTs binary composites, C1, C1.5, and C2, consist of rodlike and dotlike features dispersed in a gray/purple color background (i.e., the asphalt binder). These nanosize and micrometer-sized features are the randomly distributed CNTs coated with asphalt binders. Among them, the rodlike features (i.e., we see the length of the CNTs) highlighted in the ovals in images of C1, C1.5, and C2 are the CNTs laterally distributed close to the very top surface of the samples; the dotlike features are the cross section (i.e., we only see the diameter) of CNTs that are distributed perpendicularly to our view to different extents. Morphologies of these samples were all repeatable.

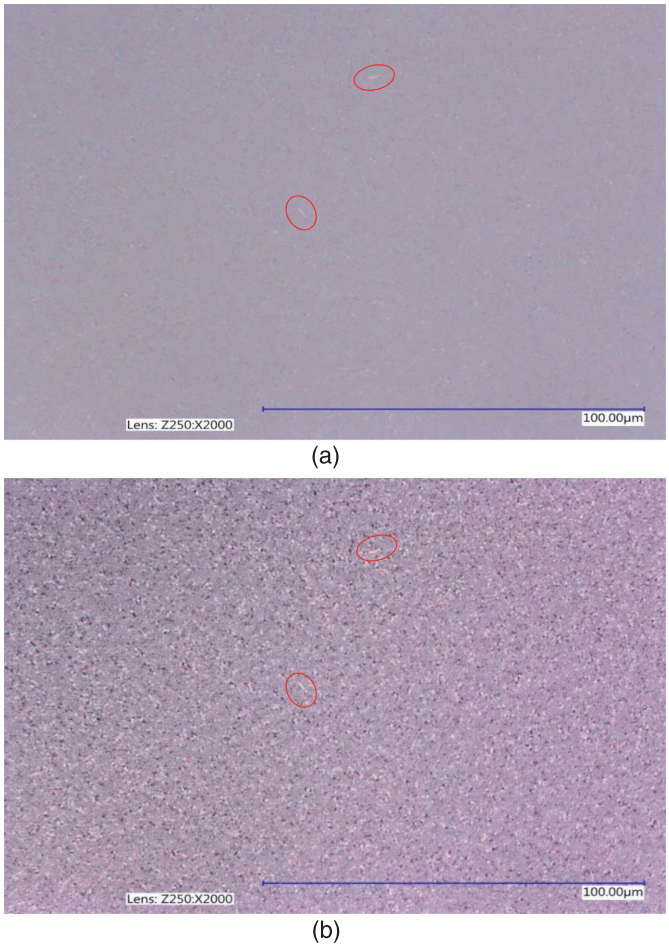

Fig. 7. Digital microscope images of C2 acquired using (a) regular recording function; and (b) HDR function.

As we expected, the area fractions of the white rods/dots increased as the CNT dosage increased; however, the change in the area fraction from C1 to C1.5 is more obvious than that from C1.5 to C2. These images revealed that the CNTs were uniformly distributed in the binder, as a result of our approach of adding the CNTs into the binder (i.e., pretreating the CNTs with the surfactant and the subsequent sonication and then mixing the CNT solution into the binder using the mechanical shear mixer and the oil bath).

Digital Microscope Images of Binders Modified with GNPs Only

Digital microscope HDR images of surfaces of G10C0 and G15C0 (i.e., binders modified with 10% and 15% by weight of GNP, respectively) are very different from those of the binder/CNTs binary composites. Figs. 9(a and b) show that surfaces of the binder/GNPs binary composites displayed colorful diffraction patterns. These patterns have a lateral size of less than 3–4μm, indicating that they are the GNP flakes [Fig. 4(b)] coated by the asphalt binder. The random distribution of the GNPs in these samples suggests that our mixing method was effective to attain a uniform dispersion of GNPs in binders.

Visually, a slightly larger amount of small-size features is observed on the surface of G15C0 compared with that of G10C0. The area fraction of the diffraction patterns on the surface of G15C0 appears to be relatively higher than that of G10C0 because the former had 5% by weight more GNP than the latter; however, the difference is not significant. This can be explained as follows: (1) the HDR images only reflect the dispersion of the GNPs near the surface of the binder, not in the bulk of the sample; and (2) GNPs are two-dimensional by nature, and they can fill a surface easily, making it difficult to tell the difference in area fraction when the GNP dosage reaches a certain value.

Digital Microscope Images of Binders Modified with Both GNP and CNT

Digital microscope HDR images of the surface morphologies of the asphalt binders/GNPs/CNTs ternary composite are similar to those of the binder/GNPs binary composite. Figs. 9(c and d) show the surface morphologies of G10GC1.5 and G15GC1.5, and images of other samples are not shown because of the similarity. Randomly distributed colorful diffraction patterns of different sizes dominate the surfaces of the ternary composites. The diffraction patterns are the GNPs and CNTs coated with the binder, and their random distribution endorses the uniform distribution of these additives in the binder.

Morphologies of the ternary composite have more similarities to those of the binder/GNPs composite than those of the binder/CNTs composite because of the unique differences in shape and size between CNTs and GNPs (i.e., rodlike versus flakelike). When comparing surface morphologies of the binder/GNPs/CNTs ternary composite with those of the binder/GNPs binary composite, more colorful patterns (especially the ones in smaller sizes) were observed in the former than the latter. This can be attributed to the addition of the CNTs; however, it is challenging to distinguish the CNTs from the GNPs in the morphologies of the ternary composite because the nanosized CNTs are blended in the two-dimensional (2D) microsized GNPs (one can imagine the difficulty of finding needles among bran flakes).

Thermal Conductivity

The morphologies of the CNT- and/GNP-modified binders revealed that the GNPs and CNTs were uniformly distributed in the binders. Therefore, enhancement in the thermal conductivity of these modified binders is expected.

Fig. 10 shows the thermal conductivity results of the control binder and the binders modified with various content of the single filler (i.e., CNTs or GNPs) and double fillers (i.e., CNTs and GNPs) at 40°C. The control sample, C0, had a thermal conductivity of 0.27 W/mK, which is comparable to values reported by other researchers (Pan et al. 2014). Fig. 10(a) shows that the presence of CNTs increased the thermal conductivities of the binder/CNT composites, with the enhancement depending on the content of the CNT. The thermal conductivities of C1, C1.5, and C2 were 29%, 35%, and 42% higher than that of C0, respectively. As for the binder/GNP binary composites, G10C0 and G15C0, their thermal conductivities were 56% and 60% greater than that of C0, respectively.

The enhancement in thermal conductivity of the GNP-modified binders in this study is comparable to that reported by Pan et al. (2014) for asphalt binders modified with graphite at the same weight fractions. When comparing the effect of CNTs with that of the GNPs on binders' thermal conductivity, the data revealed that the enhancement effect on the binder's thermal conductivity from the much higher weight fractions of GNPs (i.e., 10% and 15% by weight) is only slightly better than that of the CNTs (i.e., 1%, 1.5%, and 2% by weight).

Fig. 10(b) shows that with CNTs and GNPs both added, thermal conductivities of the ternary composites were barely (for 10% by weight GNP series) or only slightly (for the 15% by weight GNP series, by only 7%) higher compared with their respective binary base (i.e., G10C0 and G15C0). That is, the combination of the two

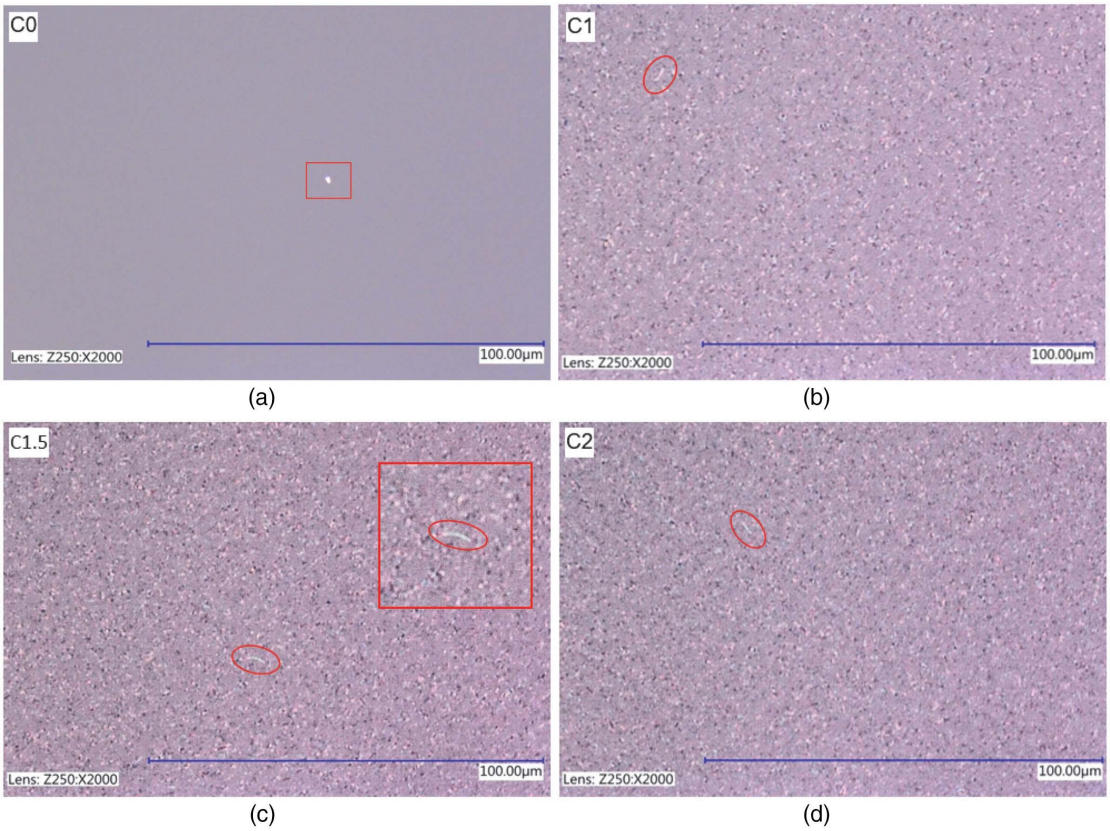

Fig. 8. Digital microscope images of C0, C1, C1.5, and C2.

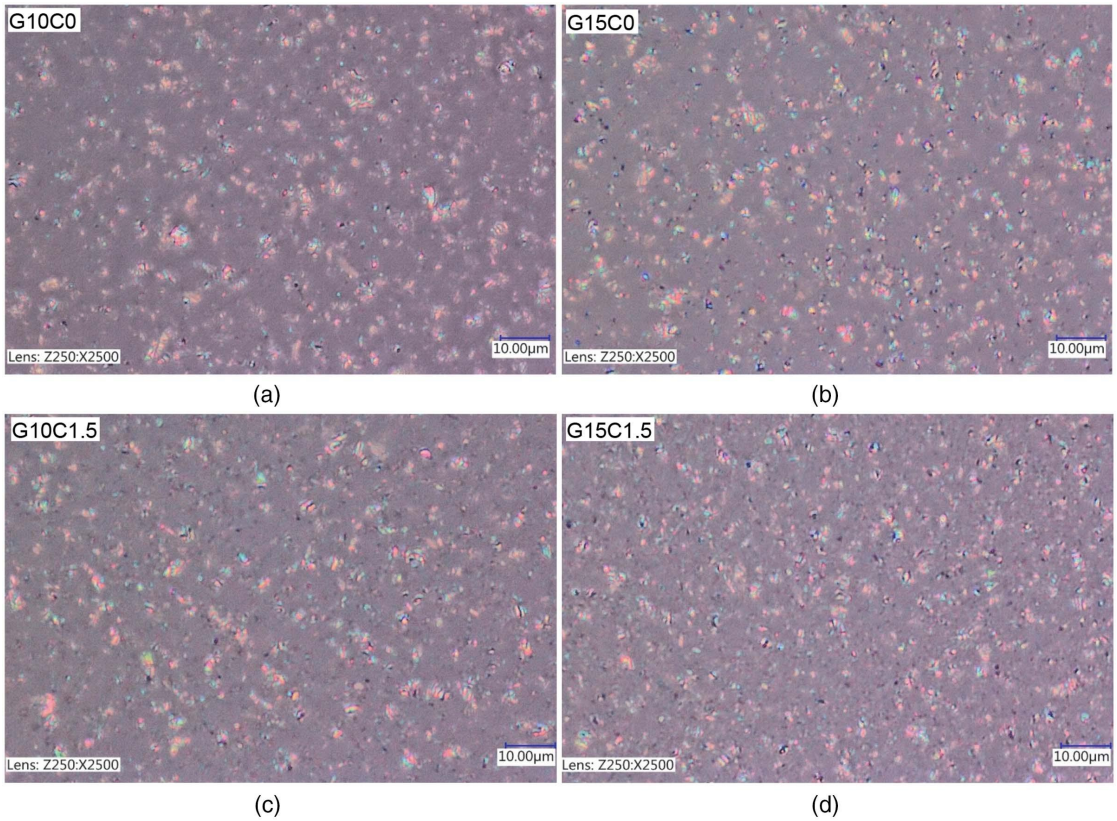

Fig. 9. Digital microscope HDR images of G10C0, G15C0, G10C1.5, and G15C1.5. The colorful diffraction patterns in sizes smaller than 3–4 μm are the GNP flakes and CNTs coated with asphalt binder.

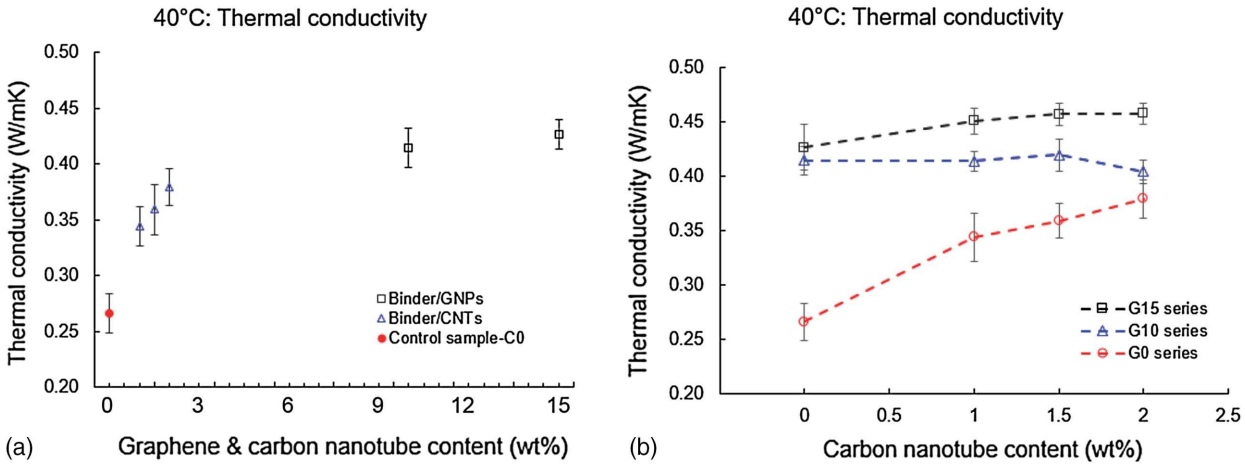

Fig. 10. Thermal conductivity at 40°C of (a) pure binder and the binary composites; and (b) all asphalt binders including pure binder, the binary, and ternary composites.

additives did not considerably boost the thermal conductivity of the asphalt binder when compared with the binder/GNP binary composites. This trend seems to be somewhat different from the findings of Che et al. (2017) and Vo and Park (2017); however, no direct comparison shall be made between our study and these two studies. Specifically, Vo and Park (2017) reported the thermal conductivity of the conductive-filled modified-asphalt concrete rather than asphalt binder; Che et al. (2017) used high-density polyethylene rather than asphalt binder as the matrix. For a more detailed comparison, the data from the thermal conductivity test are provided in Table 3.

Overall, within our experimental matrix, the highest thermal conductivity by adding CNTs and/or GNPs was from G15C2, namely 0.46 W/mK, which is 72% greater than that of the control sample, C0. The improvement in thermal conductivity by adding CNTs and GNPs is comparable to that found in other studies (Pan et al. 2014). However, the enhancement in thermal conductivities of the modified binders falls far short of our expectation considering that the thermal conductivities of pure CNTs and pure GNPs could be as high as 3,000–7,000 and 300 W/mK, respectively. This seems to be counterintuitive to the fact that the CNTs and GNPs were already uniformly dispersed in the binders. However, previous studies reported that there are many factors other than just the dispersion uniformity of the additives in the matrix that contribute to the effective enhancement in the thermal conductivity of polymer-based composites (Alig et al. 2012; Li et al. 2017).

Possible reasons for the meager improvement in the thermal conductivity of the modified binders include the high binder/CNT and binder/GNP interface resistance, thermal conductivity loss of the CNTs due to their waviness, random distribution of CNTs (rather than well-aligned), and the commercial dispersant that was used to facilitate the separation of the CNTs and GNPs (Han and Fina 2011). More importantly, it is possible that the CNTs and/or GNPs in the binders did not form interconnecting networks suitable for heat transfer in the binder because of either the not-high-enough dosages (Bai et al. 2015; Che et al. 2017; Pan et al. 2014; Vo and Park 2017) of the CNTs and/or GNPs used in this study or the choices of the specific CNTs and GNPs (e.g., dimensions and other variations in the production processes of these additives). However, we do not have a proper tool to directly observe the state of the interconnecting conductive network in the binder yet.

The highest dosages for CNTs and GNPs we used were 2% and 15% by weight, which convert to volume percentages of 0.98% and 6.44%, respectively. In fact, researchers reported a thermal conductivity enhancement of more than 3,000% for an epoxy modified with 25% GNPs by volume, where the conductive GNP network most likely had been formed (Yu et al. 2007). However, such a high dosage of GNPs means a high added cost to the asphalt industry, which might not be feasible from the economic point of view.

Table 3. Effect of CNT/GNP additives on the measured thermal conductivity of the samples

Sample name	Additives of GNP and CNT (% by weight)	Thermal conductivity (W/mK)	Increase (%)
C0 (control sample)	0, 0	0.266	N/A
C1.0	0, 1	0.345	29
C1.5	0, 1.5	0.359	35
C2.0	0, 2	0.379	42
G10C0	10, 0	0.415	56
G15C0	15, 0	0.427	60
G15C1.0	15, 1	0.451	69
G15C1.5	15, 1.5	0.457	72
G15C2.0	15, 2	0.458	72

Rheology

Fig. 11 shows the rheological properties of C0, and the binder/GNP binary samples (i.e., G10C0, and G15C0). The addition of 10% and 15% by weight of GNPs only slightly increased the binder's loss modulus G'' and phase angle δ, with rarely noticable change in elastic modulus G' and relatively more noticeable increase in complex viscosity η^* across the tested frequency range. Master curves of these samples all conformed well to the time-temperature superposition principle, except that the phase angle data in the intermediate frequency range were relatively noisier than those at the lower and higher ends.

For the binder/CNT binary composites (Fig. 12), as the CNT concentration increased from 0% to 2% by weight, loss modulus G'' did not change much, and the elastic modulus G' did not show much variation except some slight increase at the lower-frequency range. These trends in loss moduli and elastic moduli led to a slight decrease in phase angle δ. Negligible variations were seen in the complex viscosity η^* of the binders as the CNT concentration increased.

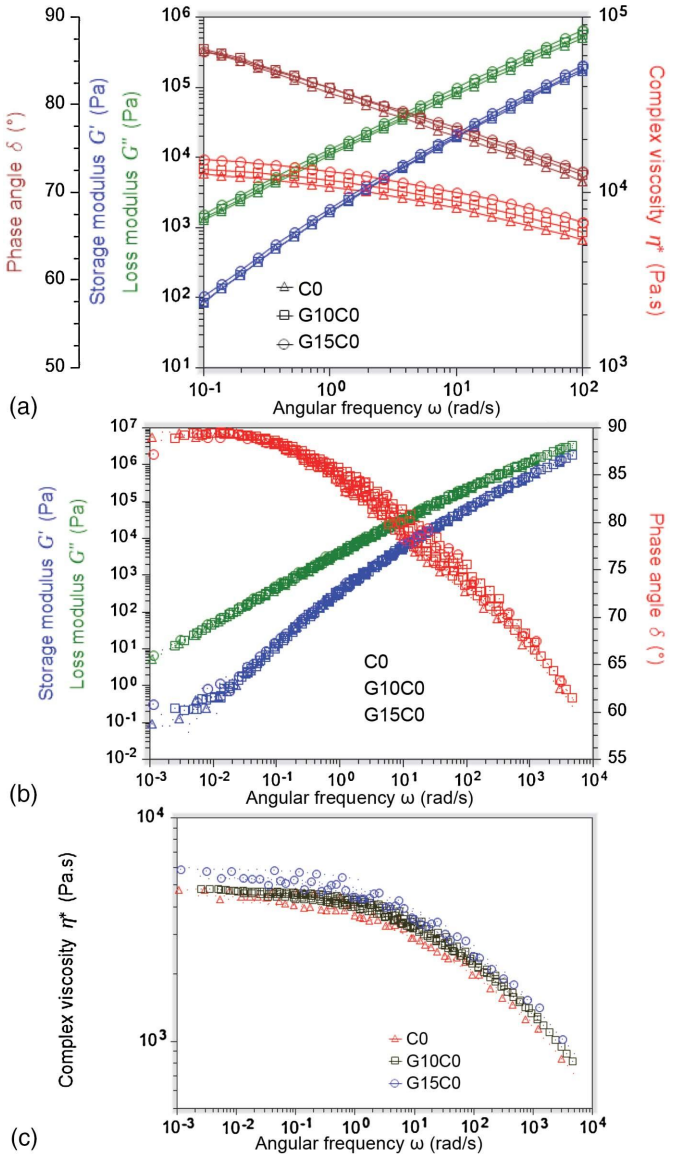

Fig. 11. Rheological properties of C0, G10C0, and G15C0: (a) δ, G', G'', and η^* at 40°C; mastercurves for (b) G', G'', and δ; and (c) η^* with a reference temperature of 46°C.

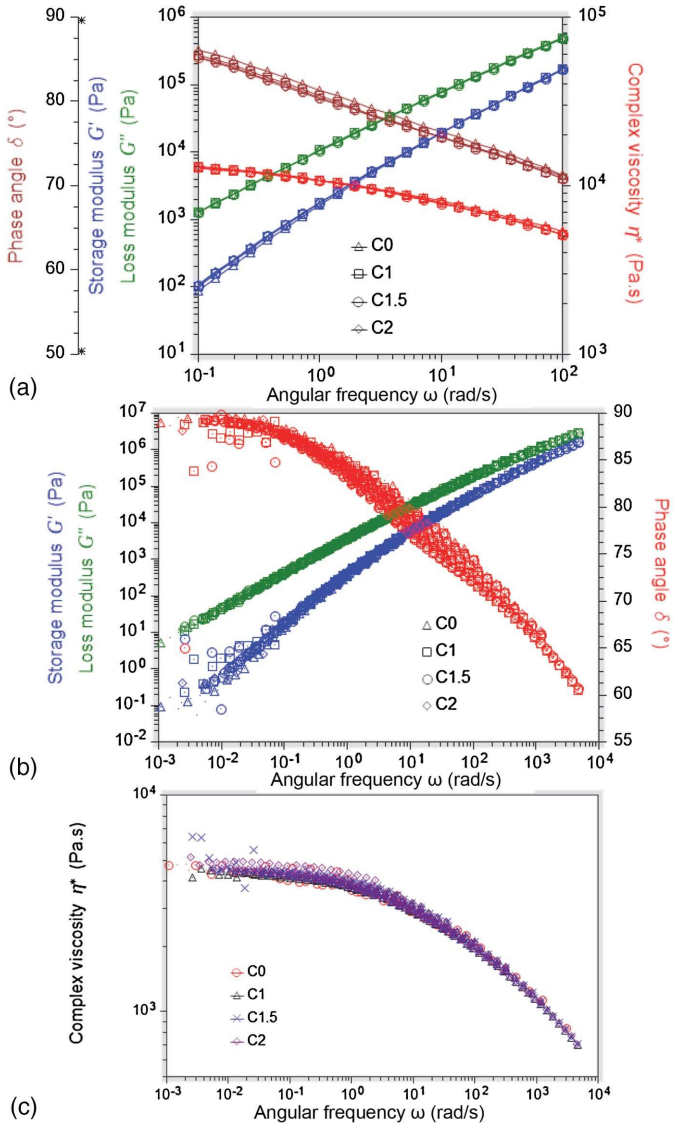

Fig. 12. Rheological properties of C0, C1, C1.5, and C2: (a) δ, $\prime$, G'', and η^* at 40°C; mastercurves for (b) G', G'', and δ; and (c) η^* with a reference temperature of 46°C.

For the G10 series (Fig. 13), as CNT concentration increased from 0% to 2% by weight, G'' mostly overlapped with each other and G' increased slightly, with a more noticeable increase in the lower frequency range, leading to a decrease in phase angle δ. As the CNT dosage increased, η^* increased, especially at the lower- and intermediate-frequency range.

For the G15 series (Fig. 14), as CNT concentration increased from 0% to 2% by weight, both G'' and G' increased, with a more significant increase seen in G' than in G'', leading to a decreasing trend in phase angle δ. Complex viscosity η^* increased with the increasing CNT dosage, especially at the lower- and intermediate-frequency ranges. More evident changes occurred to G', G'', δ, and η^* when the CNT weigh percentage increased to 2% compared with other lower CNT dosages. This suggests that the highest CNT dosage (i.e., 2% by weight of the binder) possibly resulted in more microstructural change and the consequent rheological variation in G15C2 compared with those modified with lower CNT concentrations. However, such microstructural differences are difficult to assess in the morphological images obtained from the digital microscope.

Overall, the addition of no more than 1.5% by weight CNTs and/or no more than 10% by weight GNPs did not cause significant changes to the binders' rheological properties including G', G'', and δ. For the binder/GNP binary samples, complex viscosity η^* increased as the GNP concentration increased. Only the combination of 15% by weight GNPs and 2% by weight CNTs resulted in more apparent variations in rheology. This agrees with a previous study (Pan et al. 2014).

Thus far, there have been numerous studies on improving the rheological properties of asphalt binder by the use of modifiers such as CNTs/GNPs. In many of these papers, the authors used high percentages of CNTs and/or GNPs via the dry method, i.e., adding these modifiers directly to the asphalt binder, which, as discussed in the "Introduction," would result in aggregation and inhomogeneous dispersion of the CNTs/GNPs. Although the results show an enhancement in the strength and modulus of the binder, the negative impact on the higher viscosity of the product could be a trade-off of such practices.

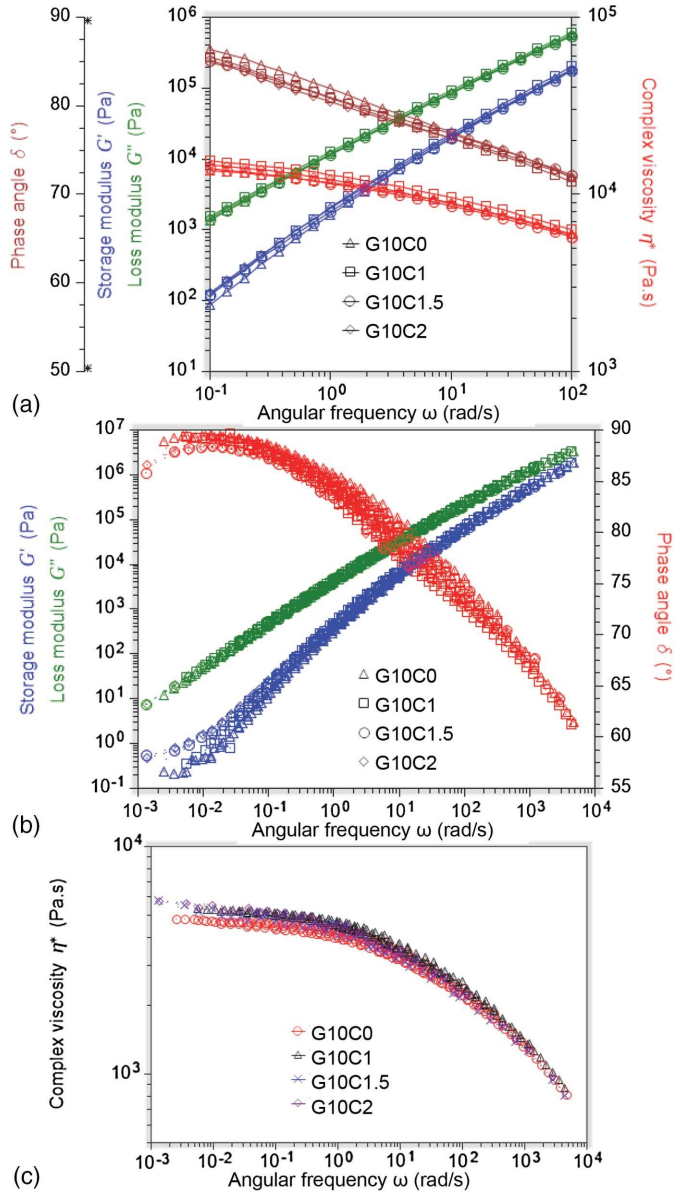

Fig. 13. Rheological properties of G10C0, G10C1, G10C1.5, and G10G2: (a) δ, G', G'', and η^* at 40°C; mastercurves for (b) G', G'', and δ; and (c) η^* with a reference temperature of 46°C.

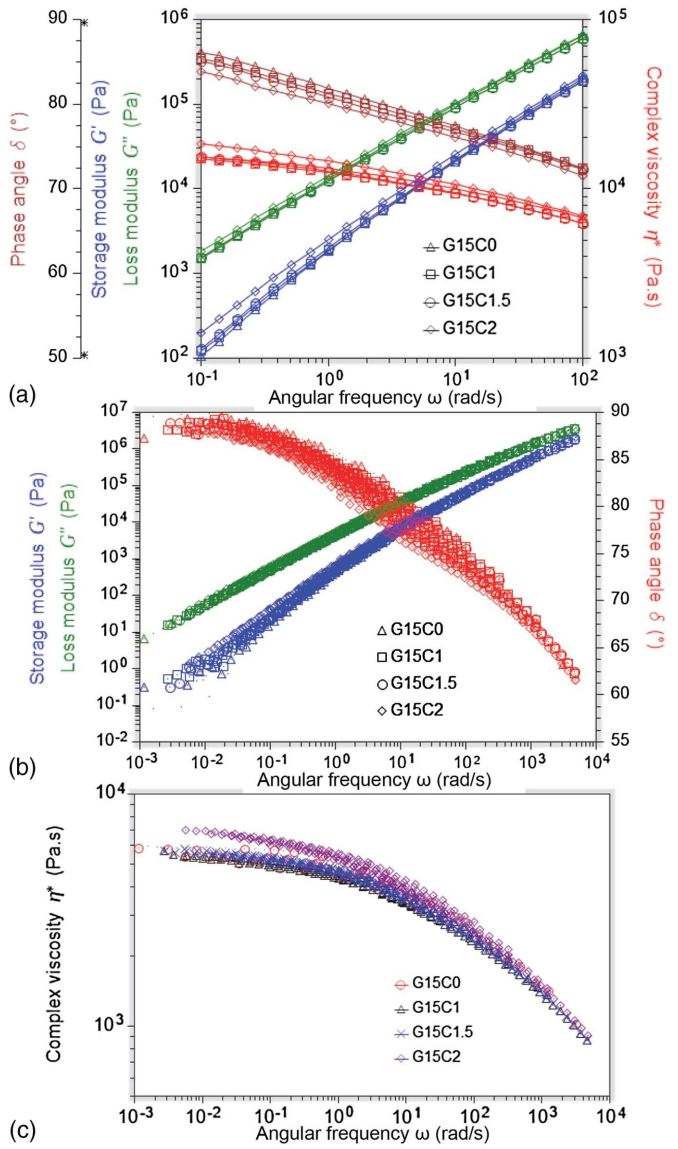

Fig. 14. Rheological properties of G15C0, G15C1, G15C1.5, and G15G2: (a) δ, G', G'', and η^* at 40°C; mastercurves for (b) G', G'', and δ; and (c) η^* with a reference temperature of 46°C.

For example, Faramarzi et al. (2015) used CNTs via both the dry method and wet method (dissolved in kerosene) to improve the rheological properties of asphalt binder. Their results for complex modulus at 60°C showed an increase of about 5.4% over the neat binder for 1% by weight of CNTs, and the data from the viscosity test at 135°C showed an increase of up to 2.5× for the dry samples and 1.2× for the wet samples. These high values of viscosity increase would result in less workability of asphalt after mixing with the aggregates, making it harder to lay down the mixture on the road.

Yang et al. (2019) investigated the effect of different percentages of CNTs and graphene on the rheological and microstructural properties of the modified binder. Their results showed a higher G^* value than the base binder for all the modified samples at lower frequencies, resulting in an improvement in the rutting resistance properties of the binder at high temperatures. However, multistress and creep recovery (MSCR) tests revealed a lower recover value (R-value) for the modified samples compared with the base binder, meaning that the modified binders had lost their elasticity and became stiffer.

In contrast to the aforementioned studies, the main goal of our study was not to enhance the rheological properties but rather to show that with the addition of low percentages of the CNTs/GNPs, the thermal conductivity can be improved, which is more important to the design and development of HAP discussed in the "Introduction," without any consequent adverse effects on the viscosity and rheological properties of the binder.

In order to perform a comprehensive study, various tests of the Superpave specification should be performed including the low-temperature cracking. However, because this paper focuses on the enhancement of the thermal conductivity of the binder for HAP, which has been discussed in the "Introduction," some tests on low-temperature properties of the binder, such as bending beam rheometer (BBR) and direct tension tester (DTT), were not performed. However, based on the results from the rheological tests of running the DSR, we can see no significant change in the storage and loss moduli of the modified binders at high frequencies (low

temperatures), which could be interpreted that although at low percentages, the CNTs/GNPs could improve the thermal properties of the binder, they do not adversely affect the rheological properties. Future performance tests can be helpful to directly show this hypothesis.

Conclusions

In this work, a more sophisticated procedure of adding the CNTs and GNPs into asphalt binders was developed, and the morphological, thermal, and rheological properties of asphalt binders modified with different dosages of CNTs and GNPs were evaluated. Some interesting findings from this study are summarized as follows:

- Compared with SEM, the digital microscope is a more proper tool to study the morphologies of CNT- and/or GNP-modified asphalt binders due to the simplicity in the sample preparation, minimum disturbance to the dispersion of the additives in the binder, and better representativeness of the true morphology. Our work directly demonstrated that the conductive coating required for SEM sample preparation of asphalt binders distorted the original microstructures of the binders for the first time.
- Digital microscopic images of the binders revealed that by pretreating the CNTs and GNPs with surfactant and sonication and then mixing the CNT/GNP solutions into the binder (heated by an oil bath) using a mechanical shear mixer, the CNTs and/GNPs were uniformly dispersed in asphalt binders. No agglomerations or clusters of CNTs or GNPs were seen in the binders, with the evidence that the average size of the colorful diffraction patterns in GNP-modified binders was very close to that of the pristine GNPs.
- The addition of CNTs and/or GNPs improved the binder's thermal conductivity. Among all samples, the thermal conductivity of G15C2 was the highest, 72% higher than that of the control binder. However, for the weight concentrations and the choices of the CNTs and GNPS we tried, the enhancement in the thermal conductivity of the modified binders was not good enough considering the much higher thermal conductivity values of the pure CNTs and GNPs. It is possible that much higher concentrations of CNTs and GNPs can allow the formation of the interconnecting networks and therefore improve the thermal conductivity of asphalt binders more significantly. However, the higher dosages of these additives would also lead to higher costs to the asphalt and pavement industries. It is also likely that the thermal conductivity of the asphalt concrete made of these CNT- and GNP-modified asphalt binders could be much higher because of the relatively higher thermal conductivity of the aggregates.
- Regarding the cost-benefit analysis of the CNTs and GNPs used in this study, only small quantities of these additives were used in our lab work, and our analysis indicates that the additional cost from these additives are minimal. Specifically, the total of 11 g of MWCNTs used in this research costs $6.60, and the 90 g of GNPs costs $7.20. As for large-scale, real-world asphalt pavement projects (e.g., HAP), the cost-benefits analysis of using these additives is likely different from our lab research. A pilot project is necessary to provide more realistic data for the life cycle cost analysis of the HAP with extra benefits in energy harvesting.
- Regarding the rheological properties, no significant changes occurred to the elastic modulus, loss modulus, and phase angle when the CNT and/or GNP dosages were no more than 1.5% and/or 10% by weight, respectively. For the binder/GNP binary samples, complex viscosity η^* increased as the GNP concentration increased. Only the combination of 15% by weight GNPs and 2% by weight CNTs resulted in more apparent variations in rheology.

Recommended future work includes developing appropriate methods to assess the state of the interconnecting network from the CNTs and/GNPs, making asphalt concrete samples using the GNP- and/or CNT-modified binders and assessing the thermal conductivity and mechanical properties of these asphalt concrete specimens, and also exploring other approaches of improving the thermal conductivity (e.g., adding steel wool fiber, and/or other conductive, recyclable industrial waste) of the asphalt concrete for more efficient temperature regulation of pavement overlays.

Data Availability Statement

Some or all data, models, or code that support the findings of this study are available from the corresponding author upon reasonable request.

Acknowledgments

This study was sponsored by the NSF IIP 1738802, 1935773, and 1941244. The authors appreciate Dr. Liming Li from the Carleton Laboratory and Dr. Fangliang Chen from Schuco for their help with the experimental tests. The authors are also thankful for the industry mentors John Collins, James J. Purcell, Bruce Barkevich, and Dr. Nima Roohi for their consultation and Nick Dietrich and Michael Crowley from Peckham Materials Corp. for providing the asphalt binders.

References

AASHTO. 1998. *Standard specification for performance-graded asphalt binder.* AASHTO MP 1. Washington, DC: AASHTO.

Ahmad, T., and H. Khawaja. 2018. "Review of low-temperature crack (LTC) developments in asphalt pavements." *Int. J. Multiphys.* 12 (2): 169–188. https://doi.org/10.21152/1750-9548.12.2.169.

Alig, I., P. Pötschke, D. Lellinger, T. Skipa, S. Pegel, G. R. Kasaliwal, and T. Villmow. 2012. "Establishment, morphology and properties of carbon nanotube networks in polymer melts." *Polymer* 53 (1): 4–28. https://doi.org/10.1016/j.polymer.2011.10.063.

Ashish, P. K., and D. Singh. 2020. "Study on understanding functional characteristics of multi-wall CNT modified asphalt binder." *Int. J. Pavement Eng.* 21 (9): 1069–1082. https://doi.org/10.1080/10298436.2018.1519190.

Asphalt Institute. 2021. "US state binder specifications." Accessed January 10, 2021. https://www.asphaltinstitute.org/engineering/specification-databases/us-state-binder-specifications/.

ASTM. 2008. *Standard test method for determining the rheological properties of asphalt binder using a dynamic shear rheometer.* ASTM D7175-15. West Conshohocken, PA: ASTM.

ASTM. 2013. *Standard test method for thermal diffusivity by the flash method*. ASTM E1461-13. West Conshohocken, PA: ASTM.

Athukorallage, B., T. Dissanayaka, S. Senadheera, and D. James. 2018. "Performance analysis of incorporating phase change materials in asphalt concrete pavements." *Constr. Build. Mater.* 164 (Mar): 419–432. https://doi.org/10.1016/j.conbuildmat.2017.12.226.

Bai, B. C., D. W. Park, H. V. Vo, S. Dessouky, and J. S. Im. 2015. "Thermal properties of asphalt mixtures modified with conductive fillers." *J. Nanomater.* 16 (1): 255. https://doi/org/10.1155/2015/926809.

Berber, S., Y.-K. Kwon, and D. Tománek. 2000. "Unusually high thermal conductivity of carbon nanotubes." *Phys. Rev. Lett.* 84 (20): 4613. https://doi.org/10.1103/PhysRevLett.84.4613.

Cheap Tubes. 2019. "Graphene nanoplatelets." Accessed June 13, 2019. https://www.cheaptubes.com/product/graphene-nanoplatelets/.

Che, J., K. Wu, Y. Lin, K. Wang, and Q. Fu. 2017. "Largely improved thermal conductivity of HDPE/expanded graphite/carbon nanotubes ternary composites via filler network-network synergy." *Composites, Part A* 99 (Aug): 32–40. https://doi.org/10.1016/j.compositesa.2017.04.001.

Chen, F., and H. Yin. 2016. "Fabrication and laboratory-based performance testing of a building-integrated photovoltaic-thermal roofing panel." *Appl. Energy* 177 (Sep): 271–284. https://doi.org/10.1016/j.apenergy.2016.05.112.

Chen, F. L., X. He, and H. M. Yin. 2016. "Manufacture and multi-physical characterization of aluminum/high-density polyethylene functionally graded materials for green energy building envelope applications." *Energy Build.* 116 (Mar): 307–317. https://doi.org/10.1016/j.enbuild.2015.11.001.

Chen, M., S. Wu, H. Wang, and J. Zhang. 2011a. "Study of ice and snow melting process on conductive asphalt solar collector." *Sol. Energy Mater. Sol. Cells* 95 (12): 3241–3250. https://doi.org/10.1016/j.solmat.2011.07.013.

Chen, M. Z., J. Hong, S. P. Wu, W. Lu, and G. J. Xu. 2011b. "Optimization of phase change materials used in asphalt pavement to prevent rutting." In Vol. 219 of *Advanced materials research*, 1375–1378. Bäch, Switzerland: Trans Tech Publications.

Dave, E. V., S. Leon, and K. Park. 2011. "Thermal cracking prediction model and software for asphalt pavements." In *Proc., Transportation and Development Institute Congress 2011: Integrated Transportation and Development for a Better Tomorrow*, 667–676. Reston, VA: ASCE. https://doi.org/10.1061/41167(398)64.

Dawson, A. R., P. K. Dehdezi, M. R. Hall, J. Wang, and R. Isola. 2012. "Enhancing thermal properties of asphalt materials for heat storage and transfer applications." *Road Mater. Pavement Des.* 13 (4): 784–803. https://doi.org/10.1080/14680629.2012.735791.

Du, H., and S. Dai Pang. 2018. "Dispersion and stability of graphene nanoplatelet in water and its influence on cement composites." *Constr. Build. Mater.* 167 (Apr): 403–413. https://doi.org/10.1016/j.conbuildmat.2018.02.046.

Eugster, W. J., and J. Schatzmann. 2002. "Harnessing solar energy for winter road clearing on heavily loaded expressways." In *Proc., New Challenges for Winter Road Service. 11th Int. Winter Road Congress World Road Association-PIARC*. Washington, DC: National Academies of Sciences, Engineering, and Medicine.

Faramarzi, M., M. Arabani, A. Haghi, and V. Mottaghitalab. 2015. "Carbon nanotubes-modified asphalt binder: Preparation and characterization." *Int. J. Pavement Res. Technol.* 8 (1): 29–37. https://doi.org/10.6135/IJPRT.ORG.TW/2015.8(1).29.

Han, Z., and A. Fina. 2011. "Thermal conductivity of carbon nanotubes and their polymer nanocomposites: A review." *Prog. Polym. Sci.* 36 (7): 914–944. https://doi.org/10.1016/j.progpolymsci.2010.11.004.

He, X., S. Abdelaziz, F. Chen, and H. Yin. 2019. "Finite element simulation of self-heated pavement under different mechanical and thermal loading conditions." *Road Mater. Pavement Des.* 20 (8): 1807–1826. https://doi.org/10.1080/14680629.2018.1473282.

Khan, Z. H., M. R. Islam, and R. A. Tarefder. 2019. "Determining asphalt surface temperature using weather parameters." *J. Traffic Transp. Eng.* 6 (6): 577–588. https://doi.org/10.1016/j.jtte.2018.04.005.

Kinloch, I. A., J. Suhr, J. Lou, R. J. Young, and P. M. Ajayan. 2018. "Composites with carbon nanotubes and graphene: An outlook." *Science* 362 (6414): 547–553. https://doi.org/10.1126/science.aat7439.

Latifi, H., and P. Hayati. 2018. "Evaluating the effects of the wet and simple processes for including carbon Nanotube modifier in hot mix asphalt." *Constr. Build. Mater.* 164 (Mar): 326–336. https://doi.org/10.1016/j.conbuildmat.2017.12.237.

Li, R., F. Xiao, S. Amirkhanian, Z. You, and J. Huang. 2017. "Developments of nano materials and technologies on asphalt materials: A review." *Constr. Build. Mater.* 143 (Jul): 633–648. https://doi.org/10.1016/j.conbuildmat.2017.03.158.

Loomans, M., H. Oversloot, A. De Bondt, R. Jansen, and H. Van Rij. 2003. "Design tool for the thermal energy potential of asphalt pavements." In *Proc., 8th Int. IBPSA Conf.* University Park, PA: College of Information Sciences and Technology.

Lu, X., P. Sjövall, H. Soenen, and M. Andersson. 2018. "Microstructures of bitumen observed by environmental scanning electron microscopy (ESEM) and chemical analysis using time-of-flight secondary ion mass spectrometry (TOF-SIMS)." *Fuel* 229 (Oct): 198–208. https://doi.org/10.1016/j.fuel.2018.05.036.

Mallick, R. B., B.-L. Chen, and S. Bhowmick. 2012. "Harvesting heat energy from asphalt pavements: Development of and comparison between numerical models and experiment." *Int. J. Sustainable Eng.* 5 (2): 159–169. https://doi.org/10.1080/19397038.2011.574742.

Manning, B. J., P. R. Bender, S. A. Cote, R. A. Lewis, A. R. Sakulich, and R. B. Mallick. 2015. "Assessing the feasibility of incorporating phase change material in hot mix asphalt." *Sustainable Cities Soc.* 19 (Dec): 11–16. https://doi.org/10.1016/j.scs.2015.06.005.

Masson, J., G. Polomark, and P. Collins. 2002. "Time-dependent microstructure of bitumen and its fractions by modulated differential scanning calorimetry." *Energy Fuels* 16 (2): 470–476. https://doi.org/10.1021/ef010233r.

Pan, P., S. Wu, Y. Xiao, P. Wang, and X. Liu. 2014. "Influence of graphite on the thermal characteristics and anti-ageing properties of asphalt binder." *Constr. Build. Mater.* 68: 220–226. https://doi.org/10.1016/j.conbuildmat.2014.06.069.

Paredes, J., and M. Burghard. 2004. "Dispersions of individual single-walled carbon nanotubes of high length." *Langmuir* 20 (12): 5149–5152. https://doi.org/10.1021/la049831z.

US Research Nanomaterials. 2021. "Carbon nanotube dispersant/CNTs water dispersant." Accessed October 20, 2021. https://www.us-nano.com/inc/sdetail/9379.

Van Bijsterveld, W., L. Houben, A. Scarpas, and A. Molenaar. 2001. "Using pavement as solar collector: Effect on pavement temperature and structural response." *Transp. Res. Rec.* 1778 (1): 140–148. https://doi.org/10.3141/1778-17.

Vo, H. V., and D.-W. Park. 2017. "Application of conductive materials to asphalt pavement." In *Advances in materials science and engineering, 2017*. London: Hindawi. https://doi.org/10.1155/2017/4101503.

Wang, H., J. Yang, and M. Gong. 2016. "Rheological characterization of asphalt binders and mixtures modified with carbon nanotubes." In Vol. 11 of *Proc., 8th RILEM Int. Symp. on Testing and Characterization of Sustainable and Innovative Bituminous Materials*, edited by F. Canestrari and M. Partl. Dordrecht, Netherlands: Springer. https://doi.org/10.1007/978-94-017-7342-3_12.

Yang, Q., Q. Liu, J. Zhong, B. Hong, D. Wang, and M. Oeser. 2019. "Rheological and micro-structural characterization of bitumen modified with carbon nanomaterials." *Constr. Build. Mater.* 201 (Mar): 580–589. https://doi.org/10.1016/j.conbuildmat.2018.12.173.

Yu, A., P. Ramesh, M. E. Itkis, E. Bekyarova, and R. C. Haddon. 2007. "Graphite nanoplatelet−epoxy composite thermal interface materials." *J. Phys. Chem. C* 111 (21): 7565–7569. https://doi.org/10.1021/jp071761s.

Yu, X., N. A. Burnham, S. Granados-Focil, and M. Tao. 2019. "Bitumen's microstructures are correlated with its bulk thermal and rheological properties." *Fuel* 254 (Oct): 115509. https://doi.org/10.1016/j.fuel.2019.05.092.